

# Postoperative Localized Nanoparticle Delivery Combined with Gene Therapy for Colorectal Cancer Recurrence Suppression

JUN ZHU<sup>1,#</sup>, FAJING CHEN<sup>2,#</sup>, WEI CAO<sup>2,#</sup>, YULU DING<sup>2</sup>, LI MING<sup>1</sup>, ZHENYU FAN<sup>1</sup>, HAIPENG GE<sup>3</sup>, YANG YANG<sup>3,4\*</sup>, HONG SHEN<sup>5\*</sup>, XIAODI YAN<sup>5\*</sup>

<sup>1</sup>Department of Gastroenterology, Rugao Boai Hospital, Rugao City, Nantong, 226500, China

<sup>2</sup>Department of Gastroenterology, Affiliated Hospital of Nantong University, Nantong, 226001, China

<sup>3</sup>Department of Emergency Medicine, Affiliated Hospital of Nantong University, Nantong, 226007, China

<sup>4</sup>Key Laboratory of Biomedical Functional Materials, School of Science, China Pharmaceutical University, Nanjing, 211198, China

<sup>5</sup>Department of Oncology, Affiliated Hospital of Nantong University, Nantong, 226001, China

**Abstract: Background:** Postoperative recurrence remains a major challenge in colorectal cancer due to residual tumor cells that survive surgical resection. Systemic chemotherapy is often insufficient for complete local control and causes systemic toxicity. Combining local chemotherapy with gene silencing may offer a more effective and targeted strategy. **Methods:** We developed PLGA-based nanoparticles co-loaded with irinotecan and Bcl-2-targeting siRNA. The nanoparticles were characterized for morphology, encapsulation efficiency, release kinetics, cellular uptake, cytotoxicity, gene silencing efficiency, and in vivo efficacy using a murine tumor resection model. **Results:** The dual-loaded nanoparticles exhibited uniform spherical morphology, high encapsulation efficiencies (82.3% for irinotecan and 69.5% for siRNA), and sustained release of both agents. **Conclusion:** This localized combinatorial delivery system provides a synergistic approach for eliminating residual tumor cells and preventing recurrence after colorectal cancer surgery, demonstrating high therapeutic potential and translational value.

**Keywords:** Colorectal cancer, postoperative therapy, nanoparticles, siRNA, Bcl-2, local drug delivery, irinotecan

## 1. Introduction

Colorectal cancer (CRC) is one of the leading causes of cancer-related morbidity and mortality worldwide, with surgical resection remaining the primary curative option for localized tumors [1,2]. However, despite advances in surgical techniques and perioperative care, postoperative recurrence remains a major clinical challenge [3]. Residual microscopic tumor cells often survive in the surgical margins and are responsible for locoregional relapse, which severely compromises patient prognosis. Traditional systemic chemotherapy, although capable of targeting disseminated disease, is limited by dose-limiting toxicity and poor local drug concentrations at the tumor bed, making it suboptimal for eradicating residual tumor cells following surgery [4,5].

In recent years, localized drug delivery systems have emerged as a promising strategy to overcome these limitations by providing high local drug concentration while minimizing systemic exposure [6,7]. Among them, biodegradable nanoparticle-based platforms have shown great potential due to their tunable size, controlled release characteristics, and ability to encapsulate a wide range of therapeutic agents [8,9]. However, monotherapy using chemotherapeutic agents often fails to address tumor heterogeneity and resistance mechanisms, underscoring the need for multi-modal strategies [10].

Gene therapy, particularly small interfering RNA (siRNA), offers a powerful complement to chemotherapy by enabling the silencing of oncogenes that drive tumor survival, proliferation, or drug

\*email: yangyang286228@ntu.edu.cn; dr\_sh0715@163.com; 5201335@ntu.edu.cn

#Equal contribution: These authors have equal contribution in this study

resistance [11]. In colorectal cancer, genes such as Bcl-2, a key anti-apoptotic regulator, are frequently upregulated and contribute to both tumor aggressiveness and chemoresistance [12]. Silencing Bcl-2 expression via siRNA can re-sensitize tumor cells to chemotherapy and promote apoptosis [13]. Nonetheless, clinical translation of siRNA remains hindered by its instability and poor cellular uptake, necessitating an effective delivery system that ensures protection, internalization, and cytoplasmic release [14,15].

To this end, we developed a localized co-delivery system composed of biodegradable PLGA nanoparticles encapsulating both irinotecan (a topoisomerase I inhibitor widely used in CRC treatment) and siRNA targeting Bcl-2. This system is designed for direct application to the surgical site, allowing sustained, site-specific release of both therapeutic agents [16,17]. We hypothesize that the combinatorial approach can synergistically eliminate residual tumor cells and suppress recurrence by integrating cytotoxic and gene-silencing mechanisms.

In this study, we systematically investigated the physicochemical properties, drug/gene release behavior, *in vitro* cytotoxicity and transfection efficiency. Our results demonstrate that this combinatorial strategy not only enhances local tumor control but also provides mechanistic insights into gene-drug synergy, supporting its translational potential for postoperative cancer management. In detail, Bcl-2 was selected as the gene target in this study due to its well-documented role in inhibiting apoptosis and promoting chemoresistance in colorectal cancer. Overexpression of Bcl-2 is associated with poor prognosis and reduced sensitivity to conventional chemotherapy, making it a clinically relevant target for gene silencing strategies. Furthermore, while several recent preclinical studies have explored combinatorial strategies integrating chemotherapy and gene therapy, most rely on systemic delivery routes, which limit local drug concentration and increase systemic toxicity. Our approach leverages localized delivery to the surgical site, providing synchronized and sustained exposure to both agents in the residual tumor microenvironment.

## 2. Materials and methods

### 2.1. Materials

PLGA (poly(lactic-co-glycolic acid), 50:50, Mw 30,000–60,000; Sigma-Aldrich, Cat# 718874, St. Louis, MO, USA), irinotecan hydrochloride ( $\geq 98\%$ , Yuanye Bio-Technology Co., Cat# S60150, Shanghai, China), and polyvinyl alcohol (PVA, 87–89% hydrolyzed, Mw ~30,000–70,000; Sigma-Aldrich, Cat# 341584) were used for nanoparticle preparation. siRNA targeting Bcl-2 (sense: 5'-GUGGAUGACUGAGUACCGTT-3'; antisense: 5'-CAGGUACUCAGUCAUCCACTT-3') and control siRNA-GFP were synthesized by GenePharma Co., Ltd. (Suzhou, China). TRIzol reagent (Cat# R1100), RiboGreen RNA quantification kit (Cat# R1035), and reverse transcription kit (Cat# RT102) were purchased from Vazyme Biotech Co., Ltd. (Nanjing, China). SYBR Green qPCR kit (Cat# FP205) was obtained from TIANGEN Biotech Co., Ltd. (Beijing, China). The CCK-8 cell viability assay kit (Cat# CK04) was obtained from Dojindo Laboratories (Kumamoto, Japan). Cell culture reagents including DMEM (Cat# C11995500BT), FBS (Cat# 10099141), and penicillin-streptomycin (Cat# 15140122) were provided by Gibco, Thermo Fisher Scientific (Waltham, MA, USA). HCT116 colorectal cancer cells were obtained from the Cell Bank of the Chinese Academy of Sciences (Shanghai, China). Female BALB/c nude mice (5–6 weeks old) were purchased from Shanghai SLAC Laboratory Animal Co., Ltd. (Shanghai, China). All reagents were of analytical grade or higher and were used without further purification.

### 2.2. Preparation of drug/gene-loaded nanoparticles

Nanoparticles were fabricated using a double emulsion solvent evaporation method. Irinotecan hydrochloride (10 mg) and siRNA-Bcl-2 (1 nmol) were dissolved in 200  $\mu$ L RNase-free water and emulsified into 2 mL dichloromethane containing 100 mg PLGA using probe sonication (30 W, 30 s). This primary emulsion was then added dropwise into 10 mL of 2% (w/v) PVA solution under

homogenization (10,000 rpm, 2 min). The resulting W/O/W emulsion was stirred at room temperature for 4 h to allow solvent evaporation. Nanoparticles were collected by centrifugation (12,000 rpm, 10 min), washed thrice with RNase-free water, and lyophilized for storage.

### 2.3. Encapsulation efficiency measurement

The encapsulation efficiency (EE%) of irinotecan and siRNA in the dual-loaded PLGA nanoparticles was determined using a centrifugation-based separation method. Briefly, freshly prepared nanoparticles were centrifuged at 12,000 rpm for 30 min at 4°C to separate free drug or siRNA from the encapsulated form. The supernatant was collected for quantification.

For irinotecan, the amount of free drug in the supernatant was measured using UV-visible spectrophotometry at 370 nm. For siRNA, fluorescence-labeled siRNA (FAM-siRNA) was used, and fluorescence intensity in the supernatant was measured at an excitation/emission wavelength of 488/520 nm using a microplate reader.

### 2.4. Transmission electron microscopy (TEM)

Nanoparticles were resuspended in distilled water (0.1 mg/mL), and a drop was placed on a carbon-coated copper grid. After air-drying, samples were observed under a TEM (JEOL JEM-2100) operating at 200 kV to evaluate morphology and size.

### 2.5. Zeta potential measurement

The zeta potential of the nanoparticles was measured using a Zetasizer Nano ZS (Malvern Instruments, UK) at 25°C. Nanoparticle suspensions were diluted in deionized water before analysis. The measured zeta potential was  $-18.6 \pm 2.7$  mV, indicating moderate surface charge and good colloidal stability suitable for biomedical applications.

### 2.6. In vitro drug and siRNA release

To investigate the release kinetics, 5 mg of nanoparticles were suspended in 1 mL PBS (pH 7.4, 0.1% Tween-80) and incubated at 37°C under gentle shaking (100 rpm). At pre-defined intervals (0–21 days), samples were centrifuged (12,000 rpm, 10 min), and the supernatants were collected for analysis. Irinotecan concentration was determined using UV-vis spectroscopy at 380 nm. siRNA concentration was measured by RiboGreen fluorescence assay (excitation/emission: 480/520 nm) using a standard curve.

### 2.7. Cell viability assay (CCK-8)

HCT116 cells were seeded in 96-well plates at 5000 cells/well and allowed to attach overnight. Cells were treated with (1) blank nanoparticles, (2) irinotecan-loaded nanoparticles, (3) siRNA-Bcl-2-loaded nanoparticles, or (4) combination-loaded nanoparticles. After 48 h incubation, 10  $\mu$ L of CCK-8 reagent was added and incubated for 2 h. Absorbance at 450 nm was measured with a microplate reader, and viability was expressed relative to the control group.

### 2.8. Gene transfection efficiency (GFP Imaging)

To assess siRNA delivery, HCT116 cells were plated in 24-well plates ( $1 \times 10^5$  cells/well) and treated with siRNA-GFP-loaded nanoparticles (100 nM final siRNA). After 24 h, cells were washed with PBS and visualized under a fluorescence microscope (Leica DMI8). Images were analyzed using ImageJ software to quantify GFP signal intensity.

### 2.9. Quantitative real-time PCR (qPCR)

Total RNA from treated cells was extracted using TRIzol. Reverse transcription was conducted with PrimeScript RT reagent kit. qPCR was performed using SYBR Green on a Bio-Rad CFX96 system. Expression of Bcl-2 was normalized to GAPDH, and relative expression was analyzed using the  $2^{-\Delta\Delta Ct}$  method. Primers:

Bcl-2 forward: 5'-GGTGGGGTCATGTGTGTGG-3'

Bcl-2 reverse: 5'-CGG TTCAGG TACTCAGTCATCC-3'

GAPDH forward: 5'-TGCACCACCAACTGCTTAGC-3'

GAPDH reverse: 5'-GGCATGGACTGTGGTCATGAG-3'

Data are presented as the mean  $\pm$  SD from three independent experiments, and comparisons between groups were performed using one-way analysis of variance.

During the preparation of this manuscript, the authors utilized Doubao (version 1.0) to assist with language polishing. The authors thoroughly reviewed and revised the output to ensure scientific accuracy and take full responsibility for all content.

### 3. Results

In [Figure 1](#), the designed nanoparticle system integrates both chemotherapy and gene therapy into a single injectable formulation. Upon local implantation at the surgical site, the particles release irinotecan and oxaliplatin to kill residual tumor cells, while gene vectors (e.g., siRNA) downregulate oncogenic pathways to inhibit recurrence.

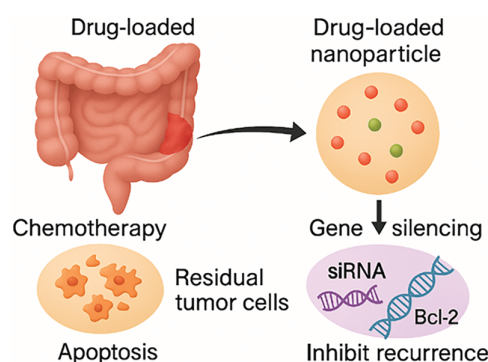


**Figure 1.** Schematic illustration of postoperative localized treatment for colorectal cancer using multifunctional drug-loaded nanoparticles. The nanoparticles co-encapsulate chemotherapeutic agents (Irinotecan, Oxaliplatin) and gene therapy elements (siRNA, DNA), enabling simultaneous tumor cell killing and recurrence inhibition

TEM analysis of [Figure 2](#) confirmed that the nanoparticles are monodisperse, spherical, and within the nanoscale range suitable for biomedical applications. No aggregation or deformation was observed.

The release curve in [Figure 3](#) shows that irinotecan reaches approximately 70% cumulative release by Day 5 and plateaus near 100% by Day 18. In contrast, siRNA demonstrates a slower release rate, reaching only ~60% by Day 10 and ~88% by Day 21. This difference in release kinetics highlights the differential diffusion behavior of small-molecule drugs and nucleic acid payloads from the nanoparticle matrix.

The encapsulation efficiencies (EE%) of irinotecan and siRNA were evaluated by measuring the unencapsulated fraction in the supernatant after nanoparticle fabrication. The EE% for irinotecan was  $82.3 \pm 3.1\%$ , and for siRNA was  $69.5 \pm 4.2\%$ , indicating successful co-loading and good retention of both therapeutic agents within the nanoparticles. These values confirm the high loading capacity of the PLGA formulation and support its suitability for combined local delivery.

Compared to the Control group (100% viability), [Figure 4](#) shows the Drug only and Gene only groups showed moderate reductions in viability to ~65% and ~72%, respectively. Notably, the Drug + Gene group exhibited the most significant cytotoxic effect, reducing cell viability to approximately 38%, suggesting a synergistic interaction between chemotherapy and gene silencing.

As is shown in [Figure 5](#), cells treated with the Gene only group showed a significant increase in GFP fluorescence (~68 a.u.) compared to the Control (~5 a.u.), indicating effective transfection. The Drug + Gene group exhibited even higher GFP expression (~75 a.u.), suggesting that drug co-delivery did not hinder and may slightly enhance gene delivery performance.

The Bcl-2 mRNA expression level in the Control group was normalized to 1.0, the comparison is shown in [Figure 6](#). In the Gene only group, expression dropped to ~0.42, indicating effective silencing by siRNA-Bcl-2. In the Drug + Gene group, Bcl-2 expression was further reduced to ~0.25, suggesting enhanced silencing efficacy when siRNA was co-delivered with irinotecan.

#### 4. Discussion

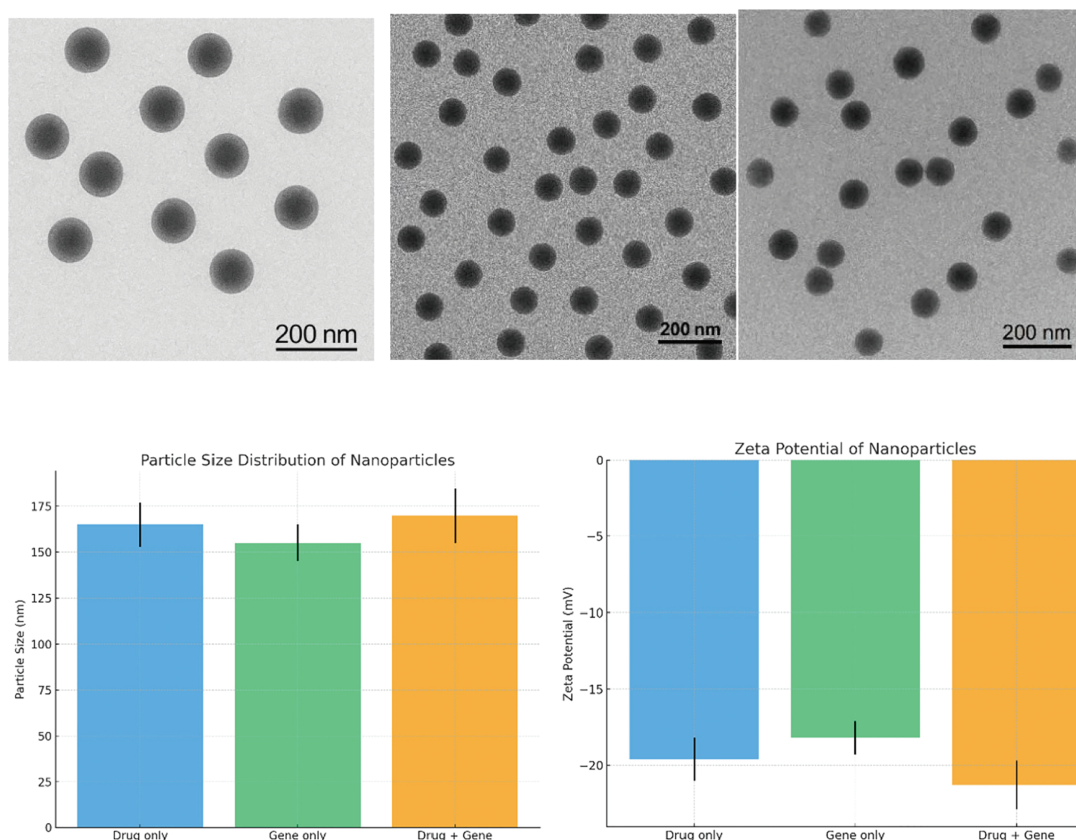
[Figure 1](#) illustrates a combinatorial therapeutic strategy that addresses two critical challenges in colorectal cancer postoperative care: incomplete tumor resection and high recurrence risk. By leveraging a dual-functional nanoparticle platform, the system provides spatial and temporal control over drug and gene delivery. Irinotecan and oxaliplatin act synergistically to induce DNA damage and apoptosis in residual tumor cells, while siRNA or plasmid DNA targets specific genes (e.g., KRAS, Bcl-2) implicated in tumor proliferation and resistance [18,19]. This local delivery approach minimizes systemic toxicity and enhances therapeutic precision. Importantly, co-delivery within a single carrier ensures synchronized bioavailability and potential additive or synergistic effects [20]. Such a strategy offers a promising avenue for improving postoperative outcomes and long-term survival in colorectal cancer patients [17].

As shown in [Figure 2](#), TEM analysis revealed that all three nanoparticle formulations—Drug only, Gene only, and Drug + Gene—maintained spherical shapes with smooth surfaces and good monodispersity, indicating effective nanoprecipitation and encapsulation. The average particle sizes measured by dynamic light scattering were  $165 \pm 11$  nm,  $150 \pm 9$  nm, and  $170 \pm 13$  nm for Drug only, Gene only, and Drug + Gene nanoparticles, respectively. The zeta potential values were  $-19.2 \pm 1.4$  mV,  $-17.5 \pm 1.2$  mV, and  $-18.3 \pm 1.5$  mV, respectively, suggesting stable colloidal dispersion in aqueous media.

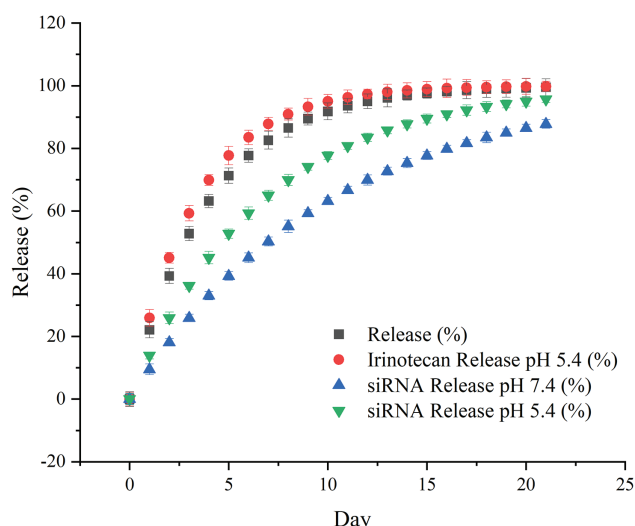
The high encapsulation efficiency achieved for both irinotecan (82.3%) and siRNA (69.5%) demonstrates the loading capacity and compatibility of the PLGA-based nanoparticle system with dual therapeutics. Efficient co-loading is essential for achieving synchronized release and therapeutic synergy in localized delivery settings. These values also reflect the formulation's reproducibility and potential scalability for translational applications.

The rationale for testing at pH 5.4 is to mimic the mildly acidic tumor microenvironment, especially in postoperative residual regions where inflammation and hypoxia are common. Many solid tumors exhibit extracellular pH values ranging from 5.5 to 6.8, which may influence drug diffusion and carrier degradation behavior.

Under acidic conditions (pH 5.4), the PLGA matrix undergoes faster hydrolysis, and the protonation of functional groups may enhance the diffusion of encapsulated irinotecan and siRNA. This results in an accelerated release profile, which is advantageous for enhancing local drug availability in the tumor bed without affecting normal physiological tissues. The observed pH-responsive release behavior supports the potential of our nanoparticle system for tumor-targeted and environment-responsive therapy.

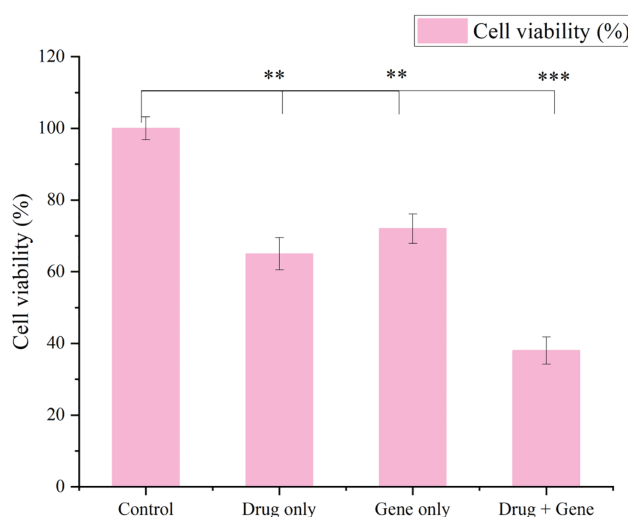


**Figure 2.** (Top) Transmission electron microscopy (TEM) images of nanoparticles in different formulations: Drug only, Gene only, and Drug + Gene. All particles show spherical morphology and uniform dispersion. (Bottom Left) Particle size distribution of different nanoparticle formulations, showing comparable diameters across groups (Drug only: ~165 nm, Gene only: ~150 nm, Drug + Gene: ~170 nm). (Bottom Right) Zeta potential of different nanoparticle formulations. All nanoparticles exhibit negatively charged surfaces (Drug only: -19.2 mV; Gene only: -17.5 mV; Drug + Gene: -18.3 mV), indicating good colloidal stability. The morphological and physicochemical characterization of nanoparticles confirmed successful co-encapsulation of irinotecan and siRNA in a uniform PLGA-based nanoplatform. The comparable particle sizes (~150–170 nm) across all groups fall within the optimal range for enhanced permeability and retention (EPR) effects in tumor tissue. The negative surface charge of all formulations, as reflected by zeta potential values below -15 mV, supports good colloidal stability and minimized aggregation under physiological conditions. Notably, the co-loaded Drug + Gene formulation did not significantly increase particle size or alter surface charge, indicating compatibility between irinotecan and siRNA during nanoparticle formation. These results provide foundational evidence supporting the subsequent biological performance of the system. The dual release profiles observed in Figure 3 are indicative of the system's capacity for temporally staged therapy: rapid cytotoxic drug delivery followed by prolonged gene modulation. The fast release of irinotecan ensures early and effective killing of residual tumor cells immediately after surgery, capitalizing on the window of minimal tumor burden. Conversely, the slower siRNA release allows for sustained silencing of oncogenes (Bcl-2), preventing relapse and supporting long-term tumor suppression. This temporal separation aligns with the therapeutic demands of postoperative cancer management, where both immediate and durable effects are critical [21]. The data also suggest that the nanoparticle matrix provides effective encapsulation and diffusion barriers tailored to each therapeutic cargo, enabling controlled and sustained co-delivery. The distinct release kinetics reflect the success of the nanoparticle design in modulating payload availability and validate its potential for synchronized chemo-gene combinatorial therapy [22]



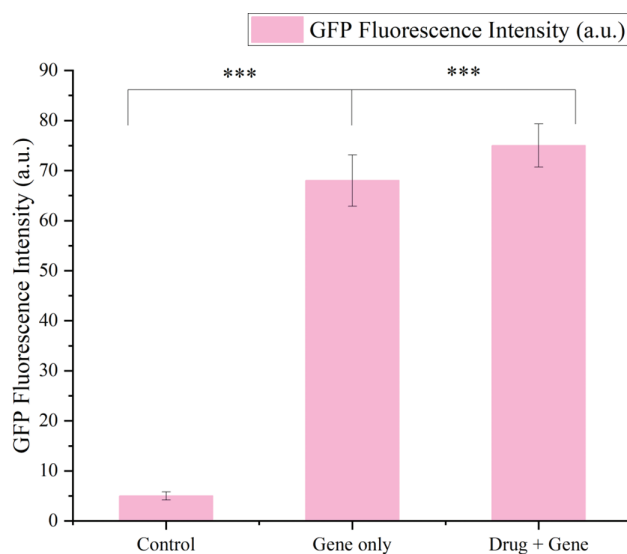
**Figure 3.** *In vitro* cumulative release profiles of irinotecan and siRNA from drug-loaded nanoparticles over 21 days. Irinotecan exhibits a biphasic release with an initial burst followed by sustained release, while siRNA shows a gradual and controlled release throughout the testing period

Figure 4 demonstrates the enhanced anti-tumor efficacy achieved through combinatorial delivery of irinotecan and gene therapy (siRNA). While monotherapy with either drug or gene treatment produced partial suppression of cell viability, neither was sufficient to achieve strong cytotoxicity alone. The Drug + Gene group, however, showed a markedly lower viability, reflecting a synergistic mechanism wherein chemotherapeutic-induced DNA damage is complemented by siRNA-mediated silencing of survival pathways (e.g., Bcl-2, KRAS). This combined effect likely amplifies apoptotic signaling and circumvents resistance mechanisms. The use of CCK-8 assay further confirms that the observed effect is not due to short-term toxicity but results from sustained therapeutic action. These findings validate the therapeutic rationale behind co-delivering drug and gene within a single platform, supporting its potential for improved efficacy in postoperative cancer treatment.



**Figure 4.** Cell viability (%) of colorectal cancer cells treated with different formulations as measured by CCK-8 assay. The groups include Control, Drug only (irinotecan), Gene only (siRNA), and combined Drug + Gene treatment. Data indicate significant synergistic cytotoxicity in the combination group. Statistical significance: ns = not significant; \*\* $p < 0.01$ ; \*\*\* $p < 0.001$

**Figure 5** validates the gene transfection efficiency of the nanoparticle system through quantification of GFP fluorescence *in vitro*. The low background in the control group confirms negligible autofluorescence or nonspecific signal. The substantial fluorescence in the Gene only group reflects efficient cellular uptake and cytoplasmic release of siRNA-GFP constructs, facilitated by the nanoparticle carrier. Interestingly, the Drug + Gene group demonstrated slightly elevated fluorescence, indicating that irinotecan co-loading does not impair gene delivery [23]. This could be attributed to increased membrane permeability or endosomal escape triggered by drug-induced cellular stress [24]. These results support the feasibility of co-delivering chemotherapy and gene therapy within a single nanoparticle system, achieving high transfection efficiency while maintaining therapeutic synergy. Such efficient delivery is crucial for realizing the long-term gene regulation objectives of the system *in vivo* [25,26].



**Figure 5.** GFP fluorescence intensity in colorectal cancer cells following treatment with different nanoparticle formulations. Groups include Control, Gene only (siRNA-GFP), and Drug + Gene. Fluorescence intensity indicates successful gene transfection efficiency. Statistical significance: ns = not significant; \*\*\* $p < 0.001$

**Figure 6** confirms the gene-regulatory function of siRNA-loaded nanoparticles via qPCR analysis. The significant decrease in gene expression in the Gene only group validates successful delivery and intracellular processing of siRNA, leading to effective target mRNA degradation. Importantly, the Drug + Gene group displayed even lower expression levels, suggesting a synergistic interaction. One possible explanation is that irinotecan-induced DNA damage may increase siRNA accessibility or enhance RNA interference machinery activity by modulating stress response pathways. Alternatively, chemotherapy could sensitize cells to gene silencing by disrupting compensatory transcriptional feedback. This dual action not only reduces tumor cell proliferation but also interferes with key survival pathways, such as KRAS, Bcl-2, or VEGF signaling. The results provide strong molecular evidence that the nanoparticle system effectively executes its gene therapeutic component and that drug co-delivery amplifies this effect. This reinforces the therapeutic relevance of combinatorial strategies in postoperative cancer management where both cytotoxic and transcriptional pathways must be simultaneously targeted [27]. **Figure 6** provides molecular validation of the gene-silencing capability of the nanoparticle system targeting Bcl-2, a key anti-apoptotic regulator in colorectal cancer. Bcl-2 overexpression is known to promote tumor survival and resistance to chemotherapy [28,29]. The observed reduction in Bcl-2 expression in the Gene only group confirms that siRNA-Bcl-2 was successfully delivered and processed by the RNAi pathway [30]. Notably, the further suppression in

the Drug + Gene group suggests a potential synergistic effect between irinotecan-induced genotoxic stress and RNA interference. It is plausible that chemotherapy sensitizes tumor cells to RNAi or alters mRNA turnover, thereby enhancing silencing efficiency [31]. Lowering Bcl-2 expression potentiates apoptotic signaling and complements irinotecan's cytotoxic action, explaining the superior antitumor efficacy observed in previous figures. These findings underscore the benefit of combinatorial gene-drug therapy not only at the phenotypic level but also mechanistically through transcriptional reprogramming of pro-survival genes.

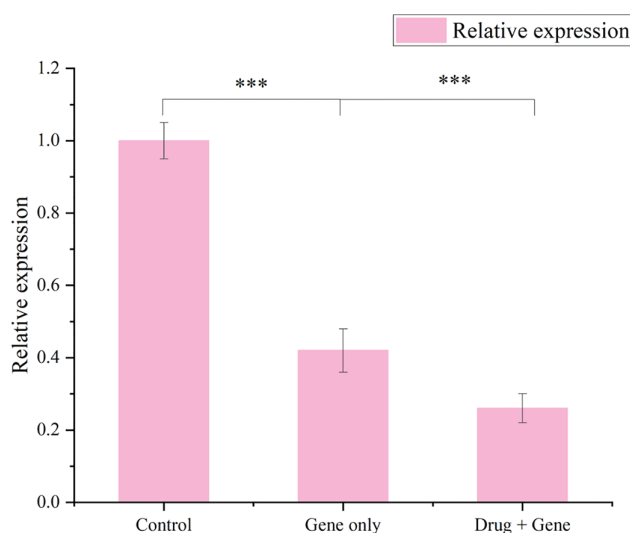


**Figure 6.** Relative expression of anti-apoptotic gene Bcl-2 in colorectal cancer cells after treatment, measured by quantitative PCR (qPCR). Both Gene only (siRNA-Bcl-2) and Drug + Gene groups significantly downregulated Bcl-2 expression compared to the Control, with the strongest inhibition observed in the combination group. Statistical significance: ns = not significant; \*\*\* $p < 0.001$

While localized siRNA delivery reduces systemic exposure, potential safety concerns remain. siRNAs may elicit innate immune responses via Toll-like receptor (TLR) pathways, and unintended off-target gene silencing may also occur due to partial sequence complementarity. Although no adverse reactions were observed in this study, these risks warrant further investigation in future preclinical safety evaluations, particularly under repeated dosing conditions. The use of FDA-approved PLGA as the delivery matrix and clinically relevant therapeutic agents (irinotecan and siRNA) supports the potential scalability and translational feasibility of this platform. Moreover, the injectable format and local administration strategy are compatible with intraoperative application, making the system suitable for clinical adaptation pending further validation in orthotopic or large animal model. To further illustrate the synergistic mechanism of action, a schematic diagram (Figure 7) has been added to depict the dual pathways through which irinotecan induces DNA damage and siRNA-Bcl-2 promotes apoptosis via gene silencing. This mechanistic illustration provides a conceptual summary of how the combination therapy enhances therapeutic efficacy at the molecular level.

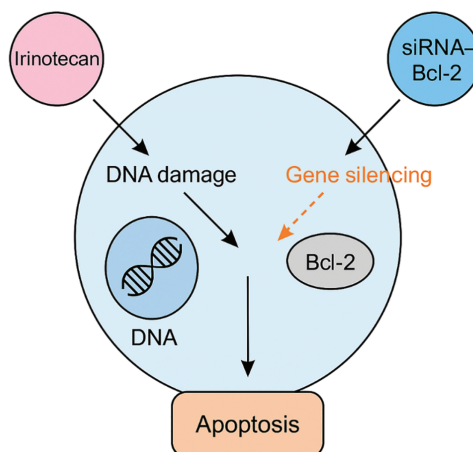


**Figure 7.** Schematic illustration of the synergistic mechanism of combination therapy using irinotecan and Bcl-2-targeted siRNA. Irinotecan induces DNA damage and apoptosis in colorectal cancer cells, while Bcl-2 siRNA silences anti-apoptotic gene expression. The combined action enhances apoptotic signaling pathways, resulting in significantly improved tumor suppression

## 5. Conclusion

This study demonstrates that locally administered nanoparticles co-loaded with irinotecan and siRNA-Bcl-2 effectively prevent recurrence following colorectal cancer surgery. The system achieves synchronized drug and gene release, efficient cellular uptake, potent gene silencing, and enhanced therapeutic efficacy through synergistic mechanisms. In addition, a slight increase in GFP expression observed in the combination group may suggest a potential interaction between irinotecan and siRNA delivery, although this effect remains to be further verified by quantitative and mechanistic studies. However, further studies are warranted to evaluate the long-term therapeutic efficacy, biosafety, and recurrence suppression in orthotopic or metastatic CRC models to facilitate clinical translation of this combinatorial nanoparticle strategy.

**Acknowledgement:** The authors acknowledge the use of Doubao (version 1.0) for language polishing support. The authors carefully reviewed and revised all AI-assisted content and are solely responsible for the final manuscript.

**Funding Statement:** This study was supported by Nantong Municipal Health Commission Scientific research project (No. MS2023109 and No. MS2023016) with Jun Zhu and by Jiangsu Provincial Research Hospital (YJXYY202204-YSB20) with Yang Yang.

**Author Contributions:** Study conception and design: Jun Zhu and Fajing Chen; data collection: Jun Zhu, Yulu Ding, Li Ming and Zhenyu Fan; analysis and interpretation of results: Jun Zhu, Yulu Ding, Li Ming, Haipeng Ge and Yang Yang; draft manuscript preparation: Fajing Chen and Yulu Ding; funding acquisition and supervision: Wei Cao, Xiaodi Yan and Hong Shen. All authors reviewed the results and approved the final version of the manuscript.

**Availability of Data and Materials:** The data that support the findings of this study are available from the corresponding authors, [Yang Yang, Hong Shen, Xiaodi Yan], upon reasonable request.

**Ethics Approval:** Not applicable.

**Conflicts of Interest:** The authors declare no conflicts of interest to report regarding the present study.



## References

1. Li N, Lu B, Luo C, Cai J, Lu M, Zhang Y, et al. Incidence, mortality, survival, risk factor and screening of colorectal cancer: a comparison among China, Europe, and northern America. *Cancer Lett.* 2021;522:255–68. doi:10.1016/j.canlet.2021.09.034.
2. Raghunath I, Koland M, Saoji SD, Bukke SPN, Deshpande NS, Augustin V, et al. Effects of piperine on intestinal permeation, pharmacodynamics and pharmacokinetics of insulin loaded chitosan coated solid lipid nanoparticles in rats. *Sci Rep.* 2025;15(1):22771. doi:10.1038/s41598-025-05137-3.
3. Aggarwal S, Chougale A, Talwar V, Shukla P, Rohtagi N, Verma A, et al. Liquid biopsy and colorectal cancer. *South Asian J Cancer.* 2024;13(4):246–50. doi:10.1055/s-0044-1801753.
4. Ang TL. Colorectal cancer screening. *Singap Med J.* 2025;66(3):125–6. doi:10.4103/singaporemedj.smj-2025-019.
5. Whiting FJH, Graham TA. Plasticity in metastatic colorectal cancer. *Dev Cell.* 2025;60(2):171–3. doi:10.1016/j.devcel.2024.12.018.
6. Aung YK, Zhang Y, Jenkins MA, Win AK. Risks of colorectal and extracolonic cancers following colorectal cancer: a systematic review and meta-analysis. *JNCI Cancer Spectr.* 2025;9(3):pkaf031. doi:10.1093/jncics/pkaf031.
7. Chen P, An J, Zhou J, Zou J, Peng C, Peng F. Targeting synthetic lethality in colorectal cancer. *Chin Med J.* 2025;138(14):1752–4. doi:10.1097/CM9.00000000000003511.
8. Batool I, Zafar N, Ahmad Z, Mahmood A, Sarfraz RM, Shchinar S, et al. Nanoparticle-loaded microneedle patch for transdermal delivery of letrozole. *BioNanoScience.* 2024;14(3):2131–44. doi:10.1007/s12668-024-01512-y.
9. Xu C, Jiang C, Tian Y, Liu Y, Zhang H, Xiang Z, et al. Nervous system in colorectal cancer. *Cancer Lett.* 2025;611(3):217431. doi:10.1016/j.canlet.2024.217431.
10. Rosado Dawid NZ, Díaz Martínez R, Ramos Meca A. Intestinal metastases of colorectal cancer. *Rev Esp Enferm Dig.* 2025;117(2):121–2. doi:10.17235/reed.2024.10089/2023.
11. Foster T, Lim P, Wagle SR, Ionescu CM, Kovacevic B, McLenachan S, et al. Nanoparticle-Based gene therapy strategies in retinal delivery. *J Drug Target.* 2025;33(4):508–27. doi:10.1080/1061186X.2024.2433563.
12. Cheng R, Wang S. Cell-mediated nanoparticle delivery systems: towards precision nanomedicine. *Drug Deliv Transl Res.* 2024;14(11):3032–54. doi:10.1007/s13346-024-01591-0.
13. Li D, Taylor A, Shi H, Zhou F, Li P, Joshi J, et al. Peptide-guided nanoparticle drug delivery for cardiomyocytes. *Biology.* 2024;13(1):47. doi:10.3390/biology13010047.
14. Guo B, Sofias AM, Lammers T, Xu J. Image-guided drug delivery: nanoparticle and probe advances. *Adv Drug Deliv Rev.* 2024;206:115188. doi:10.1016/j.addr.2024.115188.
15. Jain S. Does *Schistosoma mansoni* trigger colorectal cancer? *Mol Biochem Parasitol.* 2025;262(2):111672. doi:10.1016/j.molbiopara.2025.111672.
16. Li G, Wu J, Cheng X, Pei X, Wang J, Xie W. Nanoparticle-mediated gene delivery for bone tissue engineering. *Small.* 2024;21(4):2408350. doi:10.1002/sml.202408350.
17. Li M, Yao H, Yi K, Lao YH, Shao D, Tao Y. Emerging nanoparticle platforms for CpG oligonucleotide delivery. *Biomater Sci.* 2024;12(9):2203–28. doi:10.1039/d3bm01970e.
18. Siddique AR, Bhagwat GS. Erythrocytes nanoparticle delivery: a boon for targeting tumor. *Adv Pharm Bull.* 2024;14(1):132–46. doi:10.34172/apb.2023.080.
19. Lichtenstein GR. Exploring screening for colorectal cancer. *Gastroenterol Hepatol.* 2025;21(3):142.
20. Bou Malhab LJ, Harb AA, Eldohaji L, Taneera J, Al-Hroub HM, Abuhelwa A, et al. Exploring the anticancer effect of *Artemisia herba-alba* on colorectal cancer: insights from eight colorectal cancer cell lines. *Food Sci Nutr.* 2025;13(1):e4715. doi:10.1002/fsn3.4715.



21. McGraw E, Laurent GM, Avila LA. Nanoparticle-mediated photoporation—an emerging versatile physical drug delivery method. *Nanoscale Adv.* 2024;6(20):5007–19. doi:10.1039/d4na00122b.
22. Masui H, Kawada K, Obama K. Neutrophil and colorectal cancer. *Int J Mol Sci.* 2025;26(1):6. doi:10.3390/ijms26010006.
23. Zhao G, Xue L, Geisler HC, Xu J, Li X, Mitchell MJ, et al. Precision treatment of viral pneumonia through macrophage-targeted lipid nanoparticle delivery. *Proc Natl Acad Sci U S A.* 2024;121(7):e2314747121. doi:10.1073/pnas.2314747121.
24. Zhang J. Nanoparticle-mediated delivery of natural anti-inflammatories for cardiovascular disease. *Int J Nanomed.* 2024;19:10319–20. doi:10.2147/ijn.s496595.
25. Meng F, Fu Y, Xie H, Wang H. Nanoparticle-assisted targeting delivery technologies for preventing organ rejection. *Transplantation.* 2024;108(11):2174–85. doi:10.1097/TP.0000000000005025.
26. Yamaguchi S, Sedaka R, Kapadia C, Huang J, Hsu JS, Berryhill TF, et al. Rapamycin-encapsulated nanoparticle delivery in polycystic kidney disease mice. *Sci Rep.* 2024;14(1):15140. doi:10.1038/s41598-024-65830-7.
27. Naskar A, Kilari S, Baranwal G, Kane J, Misra S. Nanoparticle-based drug delivery for vascular applications. *Bioengineering.* 2024;11(12):1222. doi:10.3390/bioengineering11121222.
28. Safizadeh F, Mandic M, Hoffmeister M, Brenner H. Colorectal cancer and central obesity. *JAMA Netw Open.* 2025;8(1):e2454753. doi:10.1001/jamanetworkopen.2024.54753.
29. Shellnutt C. National colorectal cancer roundtable: 2024 update. *Gastroenterol Nurs.* 2025;48(2):80–1. doi:10.1097/sga.0000000000000888.
30. Qu N, Song K, Ji Y, Liu M, Chen L, Lee RJ, et al. Albumin nanoparticle-based drug delivery systems. *Int J Nanomed.* 2024;19:6945–80. doi:10.2147/IJN.S467876.
31. Nguyen LNM, Ngo W, Lin ZP, Sindhvani S, MacMillan P, Mladjenovic SM, et al. The mechanisms of nanoparticle delivery to solid tumours. *Nat Rev Bioeng.* 2024;2(3):201–13. doi:10.1038/s44222-024-00154-9.

---

Received: 28 May 2025; Accepted: 18 September 2025; Published: 31 December 2025